

Spectral signatures of serotonergic psychedelics and glutamatergic dissociatives



Carla Pallavicini ^{a,b,*}, Martina G. Vilas ^{c,1}, Mirta Villarreal ^a, Federico Zamberlan ^b, Suresh Muthukumaraswamy ^d, David Nutt ^e, Robin Carhart-Harris ^e, Enzo Tagliazucchi ^b

^a Fundación para la lucha contra las enfermedades neurológicas de la infancia (FLENI), Montañeses 2325, C1428, AQK, Buenos Aires, Argentina

^b Departamento de Física, Universidad de Buenos Aires and Instituto de Física de Buenos Aires (IFIBA – CONICET), Pabellón I, Ciudad Universitaria (1428), Buenos Aires, Argentina

^c Max Planck Institute for Empirical Aesthetics, Grüneburgweg, 14, 60322, Frankfurt am Main, Germany

^d University of Auckland Faculty of Medical and Health Sciences, 85 Park Rd, Grafton, Auckland, 1023, New Zealand

^e Centre for Neuropsychopharmacology, South Kensington Campus London, SW7 2AZ, London, United Kingdom

ARTICLE INFO

Keywords:
 Serotonergic psychedelics
 Ketamine
 Dissociatives
 Consciousness
 Machine learning
 Magnetoencephalography

ABSTRACT

Classic serotonergic psychedelics are remarkable for their capacity to induce reversible alterations in consciousness of the self and the surroundings, mediated by agonism at serotonin 5-HT_{2A} receptors. The subjective effects elicited by dissociative drugs acting as N-methyl-D-aspartate (NMDA) antagonists (e.g. ketamine and phencyclidine) overlap in certain domains with those of serotonergic psychedelics, suggesting some potential similarities in the brain activity patterns induced by both classes of drugs, despite different pharmacological mechanisms of action. We investigated source-localized magnetoencephalography recordings to determine the frequency-specific changes in oscillatory activity and long-range functional coupling that are common to two serotonergic compounds (lysergic acid diethylamide [LSD] and psilocybin) and the NMDA-antagonist ketamine. Administration of the three drugs resulted in widespread and broadband spectral power reductions. We established their similarity by using different pairs of compounds to train and subsequently evaluate multivariate machine learning classifiers. After applying the same methodology to functional connectivity values, we observed a pattern of occipital, parietal and frontal decreases in the low alpha and theta bands that were specific to LSD and psilocybin, as well as decreases in the low beta band common to the three drugs. Our results represent a first effort in the direction of quantifying the similarity of large-scale brain activity patterns induced by drugs of different mechanism of action, confirming the link between changes in theta and alpha oscillations and 5-HT_{2A} agonism, while also revealing the decoupling of activity in the beta band as an effect shared between NMDA antagonists and 5-HT_{2A} agonists. We discuss how these frequency-specific convergences and divergences in the power and functional connectivity of brain oscillations might relate to the overlapping subjective effects of serotonergic psychedelics and glutamatergic dissociative compounds.

1. Introduction

Historically, the term ‘hallucinogen’ has been used to refer to several categories of compounds capable of eliciting marked altered states of consciousness e.g. characterized by altered perception of self, time, space and one’s surroundings, plus eyes-closed complex and vivid visual

imagery (Nichols, 2004). Within this generic category exist the more specific categories of serotonergic psychedelics (SP) and N-methyl-D-aspartate (NMDA) receptor antagonist glutamatergic dissociatives (GD²). These drugs have been investigated in humans at the molecular and systems level, as well as in terms of behavioral changes and subjective effects. Both SP and GD are valuable tools to dissect the neural

* Corresponding author. Fundación para la lucha contra las enfermedades neurológicas de la infancia (FLENI), Montañeses 2325, C1428, AQK, Buenos Aires, Argentina.

E-mail address: carlap@df.uba.ar (C. Pallavicini).

¹ Both authors contributed equally to this work.

² Even though in this study we only analyzed ketamine data, we employ the more general terminology GD under the assumption that other drugs with very similar mechanisms of action (e.g. PCP) will result in comparable large-scale changes in brain activity and connectivity.

mechanisms associated with conscious experience, and are currently being explored as potential treatments for a variety of neuropsychiatric disorders (Vollenweider and Kometer, 2010; Krystal et al., 2013; Carhart-Harris et al., 2014; Nichols, 2016). The subjective effects elicited by SP and GD, together with human neuroimaging studies of individual compounds, suggest some overlap in their effects on global brain function (Pomarol-Clotet et al., 2006; Schartner et al., 2017; Preller and Vollenweider, 2018). To date, a quantitative comparison of the neurophysiological changes associated with the acute effects of SP and GD remains to be conducted.

At the molecular level, it is known that both SP and GD elicit their pharmacological action by non-selectively binding to receptors associated with different endogenous neurotransmitters. SP (e.g. lysergic acid diethylamide [LSD], psilocybin, N,N-dimethyltryptamine [DMT], mescaline) are at least partial agonists of certain serotonin (5-hydroxytryptamine [5-HT]) receptor subtypes (González-Maeso et al., 2007; Halberstadt, 2015; Nichols, 2016), but have also been shown to bind to other receptors (Ray, 2010; Rickli et al., 2015; Rickli et al., 2016), which could influence their subjective effects (Zamberlan et al., 2018). Several animal and human studies have established agonism at 5-HT_{2A} receptors as a necessary condition for the characteristic subjective effects elicited by SP (Glennon et al., 1984; Titeler et al., 1988; Hanks and González-Maeso, 2013; Krahenmann et al., 2017a,b; Preller et al., 2017; Barrett et al., 2018; Preller et al., 2018). Activation of 5-HT_{2A} receptors by SP in turn increases levels of the excitatory neurotransmitter glutamate (Aghajanian and Marek, 1999, 1997). GD (e.g. ketamine, phencyclidine (PCP), dextromethorphan) act as non-competitive antagonists at NMDA (N-methyl-D-aspartate) receptors (Anis et al., 1983; Homayoun and Moghaddam, 2007; Stahl, 2013), also resulting in the elevation of extracellular glutamate levels (Moghaddam et al., 1997). Like SP, GD also modulate the activity of diverse monoamine transporters and opioid receptors (Stahl, 2013); in particular, it has been shown that ketamine and PCP are likely agonists at 5-HT_{2A} and dopamine D₂ receptors, with binding affinities comparable with those at NMDA receptors (Kapur and Seeman, 2002). Adding to the plausibility of the serotonergic action of ketamine, it has been reported that pre-treatment with 5-HT_{2A} inverse agonist risperidone attenuates metabolic response to ketamine (Deakin et al., 2008), even though arterial spin labeling measurements revealed the opposite effect (Shcherbinin et al., 2015). Animal studies with animals show that ketamine enhances 5-HT_{2A} receptor-mediated vasoconstriction (Park et al., 2016).

Although SP and GD have some overlapping effects in terms of their effects on glutamatergic activity, their primary molecular sites of action are different. However, the complex series of neurochemical events triggered by these drugs could result in converging changes at the systems level. Administration of SP (e.g. LSD and psilocybin) (Carhart-Harris, Erritzoe et al. 2012; Roseman et al., 2014) Palhano-Fontes et al. (2015); Carhart-Harris et al. (2016a)) and GD (ketamine) (Nieters et al., 2012; Scheidegger et al., 2012) have been shown to decrease the functional integrity of the default mode network (DMN) and increase its functional connectivity with other brain systems (Kometer et al., 2015; Tagliazucchi et al., 2016), and to reduce fronto-parietal connectivity (Muthukumaraswamy et al., 2015, 2013). Reduced broadband oscillatory power (Kometer et al., 2015; Muthukumaraswamy et al., 2013; Riba et al., 2004, 2002) has been observed following the administration of LSD and psilocybin. Such reductions are especially marked in the alpha (8–12 Hz) band. On the other hand, sub-anesthetic doses of ketamine are associated with increases in gamma and theta power in anterior regions, decreases in theta power in the posterior cortex, and decreased amplitude of low frequencies in posterior areas (Muthukumaraswamy et al., 2015). Also convergent between SP and GD were increased global connectivity (Driesen et al., 2013; Tagliazucchi et al., 2016), and increased entropy (Carhart-Harris et al., 2014; Lebedev et al., 2016; Schartner et al., 2017; Tagliazucchi et al., 2014). While a review of the current literature suggests overlapping neural effects of SP and GD, the reliability of such similarities remains hard to assess lacking quantitative comparisons of

the drugs.

We introduced a framework to quantitatively estimate the similarity of changes in brain oscillations induced by the administration of different psychoactive drugs. Brain activity under the acute effects of two SP (LSD and psilocybin) and one GD (ketamine) was recorded using magnetoencephalography (MEG). We identified changes at the source level (spectral power and functional connectivity) associated with the administration of each substance relative to a placebo following a double-blind experimental design. Next, we modeled linear relationships between the spatial patterns of the changes induced by every pair of drugs. Finally, we trained multivariate machine learning models, i.e. random forests (Breiman, 2001), to distinguish each drug from the corresponding placebo using frequency-specific features, and then evaluated the accuracy of generalizing each classifier to distinguish other drugs from the placebo conditions. Since this method relies in relative differences across regions of interest in source space, it circumvents the problem of directly comparing absolute values by means of mass univariate tests, a procedure prone to be confounded by non-comparable doses of the administered drugs. We hypothesized that spectral features associated with common molecular and subjective effects of SP and GD would be informative of general signatures of the relevant subjective effects, while others would generalize only between both SP, reflecting changes in neural activity specific to agonism at 5-HT_{2A} receptors.

2. Materials and methods

2.1. Participants and experimental design

The MEG data used in this study have been previously analyzed and reported (Muthukumaraswamy et al., 2013; Muthukumaraswamy et al., 2015; Carhart-Harris, Muthukumaraswamy et al. 2016; Schartner et al., 2017). Recordings comprised 5–7 min for 15 participants for LSD, 6–10 min for 19 participants for ketamine and 2–5 min for 14 participants for psilocybin. Recordings were also performed under the same conditions after administering a placebo (saline) following a double-blind randomized design. Participant exclusion criteria are detailed elsewhere (Muthukumaraswamy et al., 2013; Muthukumaraswamy et al., 2015; Carhart-Harris, Muthukumaraswamy et al. 2016; Schartner et al., 2017). Briefly, participants were excluded if they were younger than 21 years old, pregnant, had personal or immediate family history of psychiatric disorders, suffered from substance dependence, had a cardiovascular disease, suffered from claustrophobia, blood or needle phobia, ever presented an adverse response to a hallucinogenic drug, or if they had any medical condition rendering them unsuitable for the study. All participants had previous experience with at least one hallucinogenic drug, but not within 6 weeks of the study. For ketamine, participants were also excluded if they smoked, were female, or had a body mass index outside the range of 18–30 kg/m².

LSD and psilocybin were administered in a single dose of 75 µg and 2 mg, respectively. Given the particular pharmacodynamics of LSD, MEG recordings were performed 4 h after the infusion. For psilocybin and ketamine, MEG recordings were performed immediately after the infusion. Both LSD and psilocybin were administered via intravenous infusion. Ketamine was administered with an initial bolus of 0.25 mg/kg delivered over 1 min followed by maintenance infusion at a rate of 0.375 mg/h for 40 min.

All studies were approved by a UK National Health Service research ethics committee and participants gave informed consent. Experiments were performed in accordance with relevant guidelines and regulations.

2.2. Data acquisition and pre-processing

Participants were seated for psilocybin and lay in a supine position for ketamine and LSD. Pulse rates and blood oxygenation levels were monitored throughout all acquisitions via a probe over the left-hand index finger. Whole-head MEG recordings were made using a CTF 275-

channel radial gradiometer system sampled at 1200 Hz (0–300 Hz band-pass). An additional 29 reference channels were recorded for noise cancellation purposes and the primary sensors were analyzed as synthetic third-order gradiometers.

Recordings were band-pass filtered (1–150 Hz), downsampled to 600 Hz and segmented into epochs of 2 s. Each epoch was visually inspected, and those with gross artifacts were removed from the analysis. An automated algorithm was used to remove further epochs contaminated with muscle artifacts (Schartner et al., 2017). Independent component analysis (ICA) was applied (Fieldtrip/EEGLAB) to identify and remove residual ocular, muscle and cardiac artifacts from the data. For LSD and ketamine, the components that showed a linear correlation >0.1 with the electrooculography and electromyography electrodes were automatically removed (such components were manually identified for the psilocybin data).

Source modelling of the data was performed using the Fieldtrip toolbox (Oostenveld et al., 2011). For each participant, individual forward models were generated from their individual magnetic resonance imaging (MRI) anatomical scans (Nolte, 2003). Broadband virtual sensor time-series were constructed using a linearly constrained minimum variance beamformer (Van Veen, van Drongelen et al., 1997) at 90 cortical and subcortical regions of interest (ROIs) determined by the automated anatomical labelling atlas (AAL) (Tzourio-Mazoyer et al., 2002).

2.3. Time-frequency analysis

Time-frequency analysis was performed using Hanning windowed Fast Fourier transforms ranging between 1 and 100 Hz at 0.5 Hz frequency intervals, as implemented in the FieldTrip Toolbox (Oostenveld et al., 2011). The results were split into six canonical spectral bands: delta (1–4 Hz), theta (4–8 Hz), low alpha (8–10.5 Hz), high alpha (10.5–13 Hz), low beta (13–20 Hz) and high beta (20–30 Hz). Gamma activity was excluded from the analysis since it is prone to reflect muscular artifacts that are especially manifest under the effects of SP (Barbeau and Rossignol, 1990; Muthukumaraswamy, 2013). All analyses were carried out using MEG recordings obtained after the infusion of the drug or the placebo. For each frequency band, two tailed Student's t-tests ($p < 0.05$, Benjamini-Hochberg false-discovery rate [FDR] corrected) were conducted to contrast spectral power values of each individual drug with those of the corresponding placebo.

2.4. Functional connectivity analysis in source space

For each pair of regions in the AAL atlas, the functional connectivity between the corresponding source-localized and bandpass-filtered signals was computed as the linear correlation between the envelopes of the orthogonalized time series (Hipp et al., 2012). The orthogonalization procedure is required to remove trivial co-variability in power due to recording activity from overlapping same sources, while preserving co-variation related to the measurement of independent sources. For each temporal window, least-squares regression was used to obtain the optimal linear prediction of one signal in terms of the other. The orthogonalized signal was obtained by subtracting this prediction from the original time series (i.e. by retaining the residue of the best fit in the least-squares sense). The functional connectivity was finally determined by computing the linear correlation coefficient between the envelope of the orthogonalized time series.

2.5. Linear correlation between statistical parametric maps of drugs vs. placebo

Mass univariate tests (two-tailed Student's t-tests, FDR-corrected) were conducted for the spectral power in different frequency bands (delta, theta, low alpha, high alpha, low beta and high beta) for the comparison of drug vs. placebo. Independent tests were conducted for all

ROIs (spectral power) and for all ROI pairs (functional connectivity). After visualization of the significant differences in the comparisons of LSD, psilocybin and ketamine vs. placebo, similarities in the spatial patterns of changes in spectral content and functional connectivity were assessed by computing the linear correlation coefficient of the t-values for all pairs of drugs. Thus, high correlation implied convergent spatial distribution of t-values, suggesting that the pair of drugs affected the spectral power and functional connectivity of MEG signals in a similar way across source space.

2.6. Generalization of multivariate machine learning models between drugs

To further assess whether different drugs resulted in similar spectral power and functional connectivity changes relative to the placebo condition, we trained machine learning classifiers to distinguish LSD, ketamine and psilocybin from the corresponding placebos. We evaluated the accuracy of each classifier using a five-fold cross-validation procedure, and we subsequently applied the same classifier to distinguish a different drug from the placebo, thus testing its generalizability. This resulted in the training (for each frequency band) of three machine learning classifiers which were evaluated a total of nine times.

It is important to stress that we did not train the machine learning models to classify between pairs of drugs directly (e.g. LSD vs. psilocybin), but to classify between them and the corresponding placebo conditions. We subsequently applied the models trained for one drug to the others, assessing the level of generalizability.

Multivariate classifiers were based on random forests (Breiman, 2001) as implemented in scikit-learn (<https://scikit-learn.org/>) (Abraham et al., 2014). The random forest algorithm builds upon the concept of a decision tree classifier, where samples are iteratively split into two “branches” depending on the values of their features. For each feature a threshold is introduced so that the samples are separated in a way that maximizes a metric of the homogeneity of the class labels assigned to each branch (the algorithm stops whenever a split results in a branch where all the samples belong to the same class, or when all features were used for a split). This intuitive procedure is prone to overfitting. In particular, a noisy feature selected early in the division process can bias the whole remaining decision tree and produce suboptimal results. To attenuate this potential issue, the random forest algorithm creates an ensemble of decision trees based on a randomly chosen subset of the features. After training each tree in the ensemble, the probability of a new sample belonging to each class is determined by the aggregated “vote” of all decision trees. We trained random forests with 1000 decision trees and a random subset of features of size equal to the (rounded) square root of the total number of features. The quality of each split in the decision trees was measured using Gini impurity, and the individual trees were expanded until all leaves are pure (i.e. no maximum depth). No minimum impurity decrease was enforced at each split, and no minimum number of samples were required at the leaf nodes of the decision trees. The hyperparameters of the model are also detailed in the documentation at <https://scikit-learn.org/>.

For each frequency band, we introduced the spectral power at each of the 90 ROIs as features for the algorithm. We trained random forest classifiers to recognize each drug from the corresponding placebo, and then evaluated the performance using a five fold cross-validation procedure. In order to assess the statistical significance of the output, we trained and evaluated a total of 1000 random forest classifiers using the same features but scrambling the class labels. We then constructed an empirical p-value by counting the amount of times the accuracy of the classifier based on the scrambled labels was greater than that of the original classifier. The accuracy of each classifier was determined as the area under the receiver operating characteristic (AUC). Subsequently, the generalizability of the classifiers to distinguish other drugs from the corresponding placebos was evaluated by applying both the original and scrambled classifiers to the spectral features and constructing a p-value in a similar way.

This procedure was repeated for the functional connectivity values using two different approaches based on global and local features, respectively. In the first case, we reproduced the aforementioned procedure using the functional connectivity values as features for each frequency band and each dataset. Upon evaluation of these classifiers we estimated that $AUC > 0.7$ produced significant accuracy values ($p < 0.05$, FDR corrected). We then repeated the procedure for the functional connectivity values of each ROI (e.g. the “connectivity profile” of each region) (Passingham et al., 2002); i.e. we built 90 random forest classifiers to distinguish each drug from its placebo based on the functional connectivity of each ROI with all others. This resulted in a total of 1620 classifiers (90 per drug and frequency band), which were trained and evaluated in terms of their generalizability to other drugs. For the classifiers based on the functional connectivity values of individual ROIs, significant accuracies were determined by $AUC > 0.7$.

3. Results

We first computed the difference in spectral power between each drug and the corresponding placebo for all frequency bands. Fig. 1 shows a rendering of the source space ROIs where we observed significant differences, color-coded to indicate the level of statistical significance. When compared with placebo, all three drugs decreased spectral power in the low and high alpha bands, and in the low beta band. The intensity and location of these changes varied for the different drugs; moreover, psilocybin decreased power of high beta oscillations, while ketamine reduced power in the delta band. LSD was the only drug to produce significant decreases in all the examined frequency bands and also presented the largest effect sizes. LSD-induced spectral power decreases were spread across most brain regions, especially in the delta through high alpha bands. In all the frequency bands where we found differences (except high beta), spectral power was reduced in the bilateral thalamic ROIs.

Next, we tested the similarity of the spatial distributions of spectral power decreases between drugs using a linear model. Scatter plots of the

decreases (Student's t) for all pairs of drugs across all source space ROIs are shown in Fig. 2. Pearson's correlation coefficients (R) are shown in the insets; the dashed red line represents the best linear fit in the least-squares sense. The correlation values were generally low, implying that in most cases the changes in MEG spectral power induced by a compound vs. the placebo were not spatially similar to those elicited by other compounds. The highest similarities were observed for ketamine vs. LSD in the low alpha band ($R = 0.55$) and psilocybin vs. LSD in the theta band ($R = 0.44$). Also similar were the decreases induced by LSD vs. psilocybin in the low alpha band ($R = 0.32$) and in the delta band ($R = 0.37$), and by LSD vs. ketamine in the delta band ($R = 0.38$). All the associated p-values were significant at $p < 0.05$, FDR-corrected.

To further investigate the similarity of the spectral power decreases, we trained multivariate machine learning classifiers (random forests) to distinguish each drug from the corresponding placebo based on the spectral power at all source space ROIs. We then evaluated whether the trained models could be generalized to classify other drugs from the placebo. The results of this analysis are summarized in Fig. 3. Each node represents MEG experiments with LSD, psilocybin and ketamine, and each arrow the result of training a machine learning classifier using data corresponding to the starting node, and evaluating it using data corresponding to the ending node (only arrows representing classifiers that yielded significant accuracy, as determined by label shuffling and $p < 0.05$ FDR-corrected, are shown). We observed that for all frequency bands the classifiers trained using psilocybin data could distinguish LSD from placebo, and that for all bands (except high beta) classifiers trained using LSD data could distinguish ketamine from placebo. In both low and high alpha bands and in the low beta band the classifiers generalized with significant accuracy for almost all drug pairs.

We computed the functional connectivity between 90 source space ROIs for all frequency bands and conditions, as described in the Methods section. Fig. 4 summarizes the results, presenting the magnitude of the difference in functional connectivity between the drug and placebo conditions (in terms of Student's t-values). The pairs of regions whose functional connectivity changes significantly are shown above the

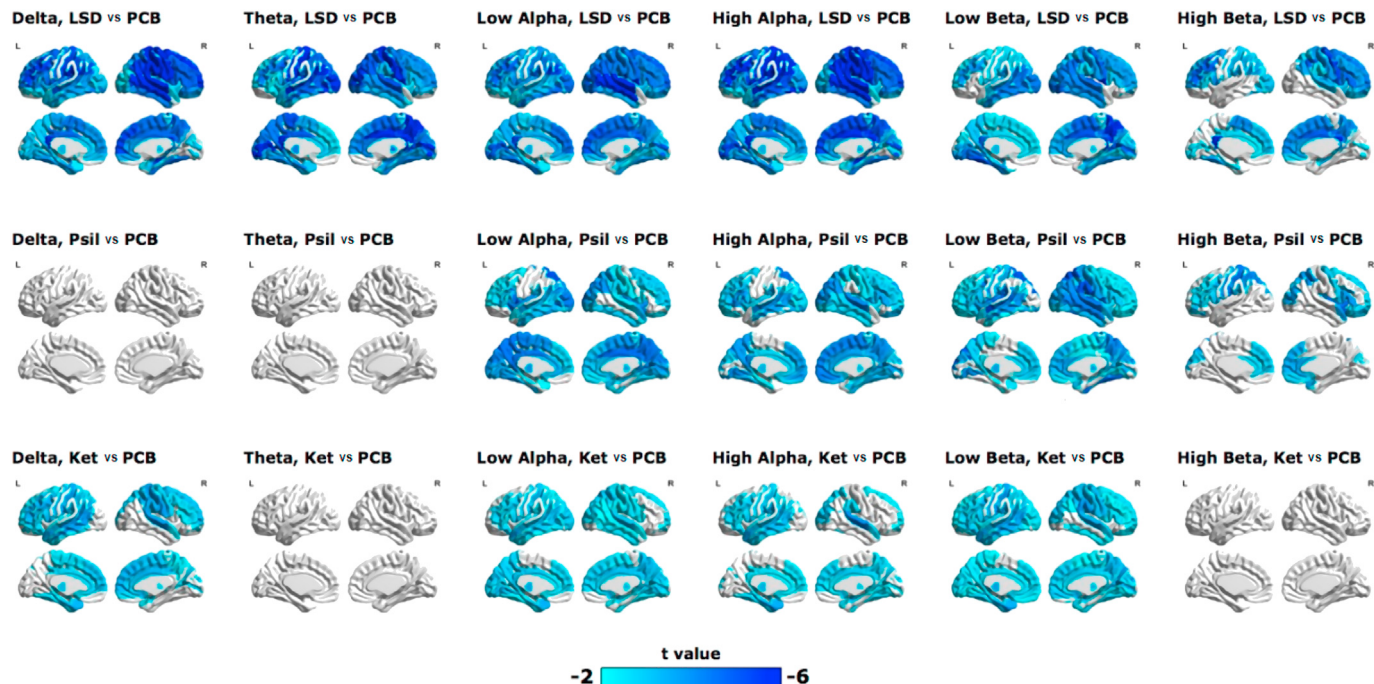


Fig. 1. Comparison of source space spectral power between the drug and placebo conditions for all frequency bands. Anatomical rendering of the brain regions displaying significant reductions in spectral power (Student's t-values, $p < 0.05$, Benjamini-Hochberg FDR-corrected). No significant increases in spectral power were observed. L: left; R: right; PCB: placebo; LSD: lysergic acid diethylamide; Psil: psilocybin; Ket: ketamine. The negative t-values indicate larger spectral power in placebo vs. drug.

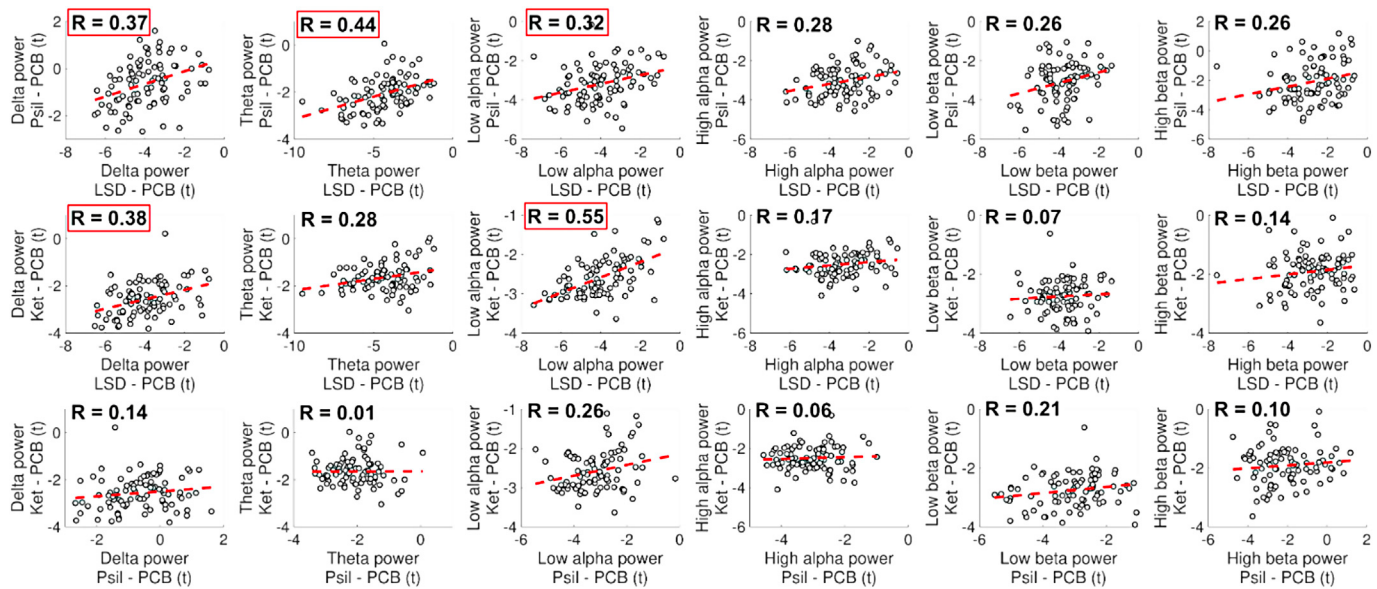


Fig. 2. Linear correlation between the spatial distributions of changes in spectral power (drug – placebo). Each point represents one of the 90 ROIs; with its x and y axis coordinates indicating the spectral power change (Student's t-values) for all pairs of drugs and all frequency bands. Dashed red lines indicate the best linear fit in the least-squares sense. Pearson's linear correlation coefficients (R) are provided as insets. PCB: placebo; LSD: lysergic acid diethylamide; Psil: psilocybin; Ket: ketamine. Correlations presenting high effect sizes are highlighted in red.

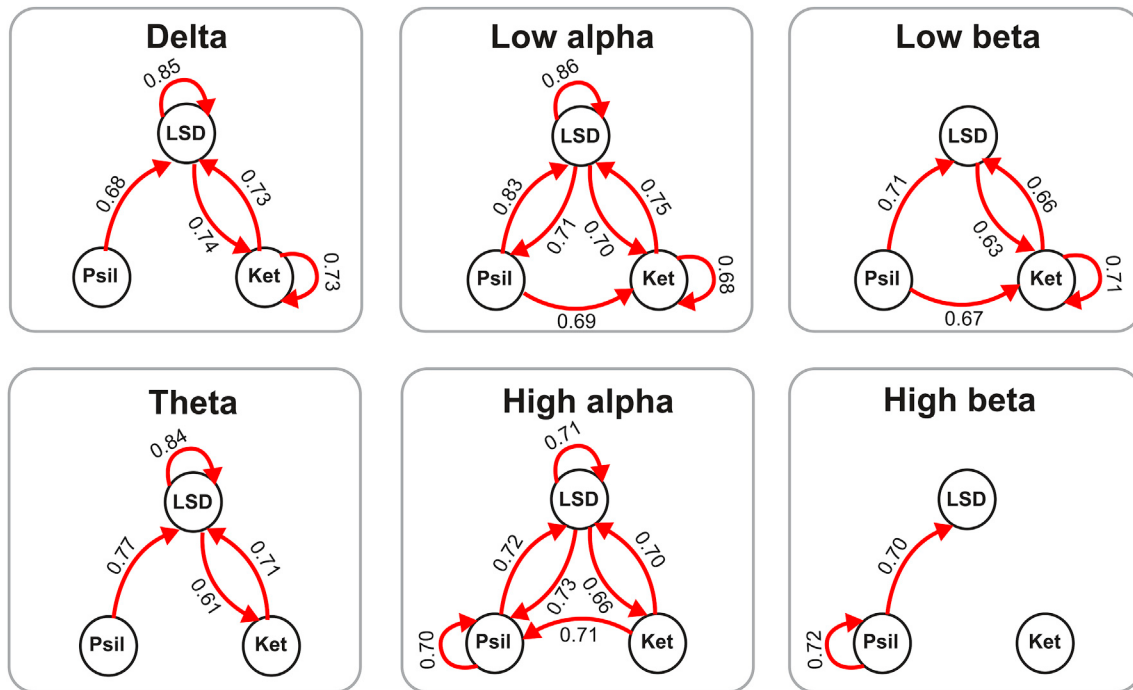


Fig. 3. Generalization of machine learning classifiers to distinguish drug vs. placebo based on the spectral power of the delta, theta, low and high alpha, and low and high beta bands. Red arrows indicate significant accuracy ($p < 0.05$, Benjamini-Hochberg FDR-corrected determined by 1000 classifiers with random label shuffling) of a random forest classifier trained to distinguish the drug indicated in the starting node and tested to distinguish the drug indicated in the ending node. The mean AUC values of each classifier are shown next to the corresponding arrows (e.g. a classifier trained to distinguish psilocybin from placebo in the theta band can also distinguish LSD from placebo with $AUC = 0.77$ and $p < 0.05$, Benjamini-Hochberg FDR-corrected). LSD: lysergic acid diethylamide; Psil: psilocybin; Ket: ketamine.

diagonal of the matrices in Fig. 4 ($p < 0.001$). LSD significantly reduced connectivity values for all the frequency bands, with the most widespread changes in low beta, followed by theta and high beta. In contrast, psilocybin and ketamine resulted in sparse functional connectivity reductions in the low and high beta bands. A network representation of the ROI pairs with the 5% highest decreases/increases of drug vs. placebo functional connectivity is shown in Fig. 5 (note that only significant

decreases in functional connectivity were detected).

In contrast to the correlation analyses using power spectrum values (Fig. 2), functional connectivity values presented positively correlated changes for several pairs of drugs in the theta and in the low and high alpha bands, as shown in Fig. 6. For instance, $R = 0.67$ was observed between psilocybin and LSD in the low alpha band; however, correlations between functional connectivity changes under ketamine vs. LSD

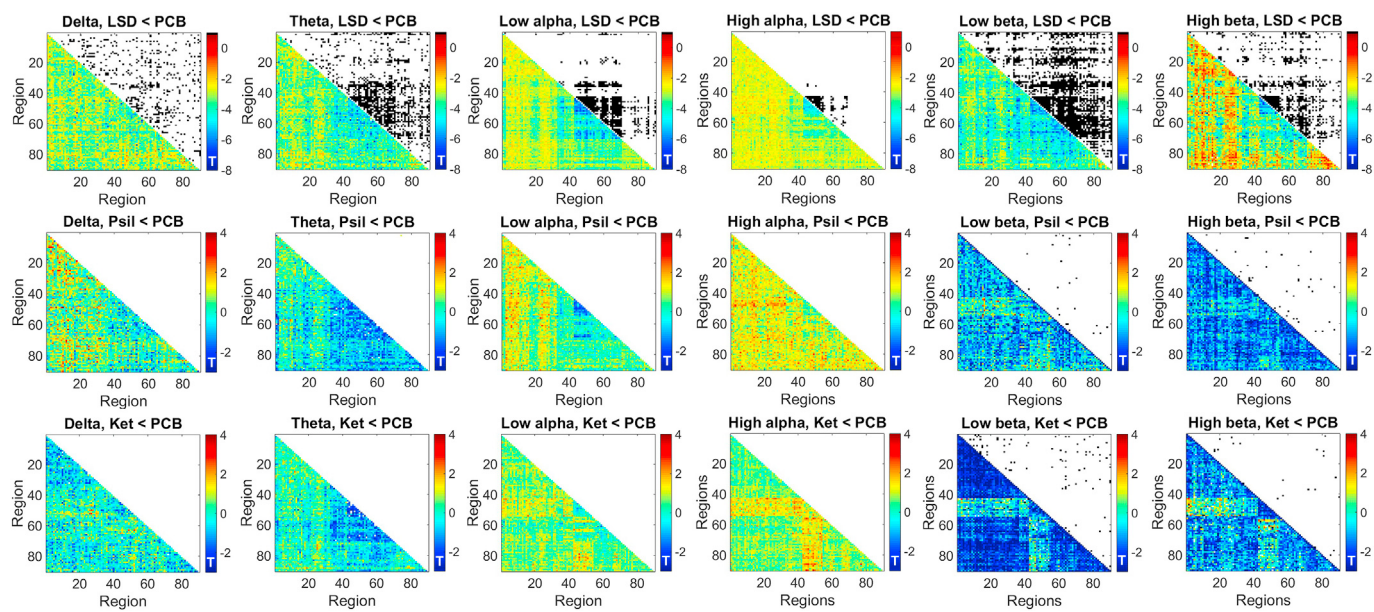


Fig. 4. Functional connectivity differences between the drug and placebo conditions. Matrices of Student's t-values (below diagonal) and statistically significant changes in functional connectivity ($p < 0.001$, uncorrected) (above diagonal) for each drug vs. placebo (rows), computed for all frequency bands (columns). PCB: placebo; LSD: lysergic acid diethylamide; Psil: psilocybin; Ket: ketamine. The negative t-values indicate larger functional connectivity in placebo vs. drug.

($R = 0.30$) and under ketamine vs. psilocybin ($R = 0.22$) were considerably lower. In addition, we observed that all the pairs of drugs displayed high correlation values ($R \geq 0.40$) in the theta band.

We then repeated the multivariate analysis based on training and evaluating machine learning classifiers using data from different compounds (as in Fig. 3). In this case, the features comprised functional connectivity values between all pairs of ROIs. Results are shown in Fig. 7. In contrast to Fig. 3, we observed less training/evaluation pairs with significant AUC values. This is consistent with the results portrayed in Fig. 4, where only LSD presented significant connectivity differences for all spectral bands; furthermore, classifiers trained and evaluated with LSD data presented significant AUC values for the frequency bands where most significant differences were observed (theta, low and high alpha, and low and high beta). In the theta, low alpha and low beta bands, random forest classifiers trained using the psilocybin data generalized to the LSD data, while most classifiers generalized to other drugs in the low beta band.

Finally, we mapped brain regions whose functional connectivity in the low alpha band (the band which presented most selectivity in the generalization between LSD and psilocybin) allowed random forest classifiers to distinguish with significant AUC the LSD data from its placebo, as well as to generalize between psilocybin and LSD. For this purpose, we implemented random forest classifiers trained and evaluated using the functional connectivity values between each individual ROI and all remaining ROIs. The results shown in Fig. 8 indicate that ROIs in the occipital lobe that allow generalization between LSD and psilocybin are also relevant for the classification between LSD and the placebo condition. Besides ROIs corresponding to the visual cortex in the occipital lobe, functional connectivity of parietal and frontal DMN nodes also resulted in significant AUC values for classifiers trained using psilocybin data and evaluated using LSD data.

4. Discussion

Different neuroimaging tools such as functional magnetic resonance imaging (fMRI) and MEG have been applied to characterize the changes in brain activity elicited by psychoactive drugs, including “classical” serotonergic psychedelics, as well as dissociative NMDA antagonists (Dos Santos, Osório et al., 2016). Despite the growing number of studies

showing promise in the application of these tools, an integrative account examining the consistency between non-invasive recordings of brain activity and the known pharmacological mechanisms of action remains to be developed. We followed this approach and showed that, while decreased spectral power and decreased source functional connectivity were landmark features common to LSD, psilocybin and ketamine, changes in specific frequency bands allowed generalization of machine learning classifiers only between LSD and psilocybin. In the following we discuss our findings in terms of previous neuroimaging experiments, the subjective effects and the mechanisms of action of these compounds, and we outline how our methodology could be extended to investigate other sources of data.

Consistent with previous findings (Carhart-Harris et al., 2016b; Kometer et al., 2015; Muthukumaraswamy et al., 2015, 2013), we found that both SP and GD decreased the power of broadband oscillations as measured with MEG. It has been argued that decreases in lower frequencies (<20 Hz), especially in the alpha band, reflect the effect of agonism at 5-HT_{2A} receptors by SP (Kometer et al., 2015). However, our results indicate that these decreases might reflect more general processes that can be caused by the action of NMDA antagonists as well, whose subjective effects share some commonalities with those of 5-HT_{2A} agonists. We note that changes in theta band spectral power did not survive multiple comparison correction. However, the application of an uncorrected statistical threshold ($p < 0.01$) revealed a pattern of posterior theta power decrease, consistent with Muthukumaraswamy et al., (2015).

Decreased power in the alpha and beta bands has been associated with cortical disinhibition processes (Klimesch et al., 2007), which in turn could account for the reported increases in entropy levels that follow the infusion of both SP and GD (Schartner et al., 2017). Multivariate analyses showed that power spectrum changes (in all frequency bands except for high beta) observed after the administration of ketamine were similar and informative of those changes elicited by LSD and vice-versa, further suggesting that broadband reductions in spectral power are a signature common to both drugs. Changes in the high beta band appeared as an exception and diverged between LSD/psilocybin and ketamine, consistent with previous reports of different spatial patterns of glucose consumption during the acute effects of SP and GD (Daumann et al., 2010) and the observation that high beta oscillations are correlated

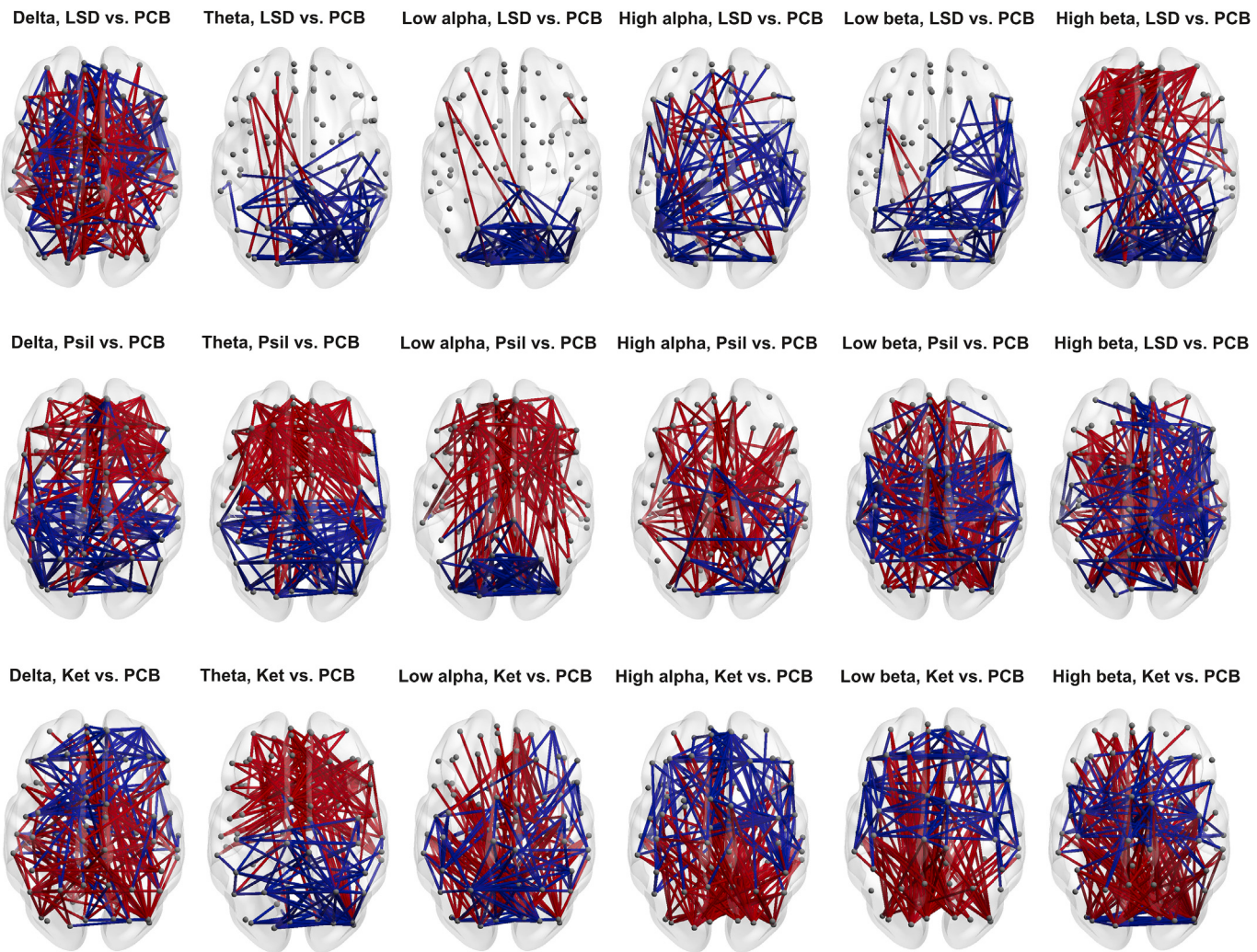


Fig. 5. Network representation of differences in source-space functional connectivity between drugs and placebo. For each drug (rows) and frequency band (columns), the top 5% positive (red) and negative (blue) entries of the difference of functional connectivity matrices are shown. PCB: placebo; LSD: lysergic acid diethylamide; Psil: psilocybin; Ket: ketamine.

with glucose metabolism (Nofzinger, 2000). It is interesting to note that simple univariate linear models did not account for the similarity of changes in spectral power elicited by SP and GD, even though a moderate positive linear correlation between ketamine and LSD-induced changes was found.

Convergences and divergences in the spectral signatures of SP and GD manifested more clearly in the analysis of functional connectivity. The similarity of the functional connectivity decreases elicited by psilocybin and LSD was evident upon visual inspection in the low alpha band (i.e. the common decreases observed in the occipital cortex) and, less markedly, in the theta band. Using different pairs of drugs for training and evaluation of multivariate models confirmed this observation. On the other hand, significant accuracies were observed for most training/evaluation pairs in the low beta band, suggesting that functional connectivity decreases in this frequency band might represent effects common to both SP and GD. To the extent that long-range synchronization between electrophysiological oscillation reflects ongoing cognitive processing (Engel et al., 2013), similarities in the beta band could represent overlapping subjective effects. Both SP and GD are known to affect consciousness of the self (Millière, 2017), resulting in distorted ego-boundaries (Lebedev et al., 2015; Tagliazucchi et al., 2016). Previous studies link self-referential processes to DMN activity (Qin and Northoff, 2011), whose hemodynamic activity correlates with the power of electrophysiological oscillations in the beta band (Laufs et al., 2003). The

three drugs here investigated resulted in broadband functional connectivity decreases, consistent with previous reports of diminished DMN connectivity elicited by psychedelics associated with the experience of ego dissolution (Carhart-Harris, Erritzoe et al. 2012; Carhart-Harris et al., 2016b, 2012b; Kometer et al. (2015); Muthukumaraswamy et al. (2013); Palhano-Fontes et al. (2015); Scheidegger et al. (2012)). Note, however, that increased global functional connectivity (measured using fMRI) of a high-level network overlapping partially with some DMN regions was found to correlate positively with the self-reported intensity of ego dissolution under LSD (Tagliazucchi et al., 2016) – suggesting that while the DMN may locally disintegrate under SPs, it may also globally integrate. Future studies should investigate whether alterations in self-awareness underlie some of the shared spectral signatures of SP and GD.

Differences in the subjective effects elicited by low to moderate doses of ketamine and SP appear in the quality and intensity of sensory alterations, mainly in the visual domain (Vollenweider and Kometer, 2010). Visual distortions have been associated with alpha activity (Carhart-Harris et al., 2016b), and different authors have independently proposed that psychedelic-induced visual imagery reflects reduced cortical inhibition, resulting in spontaneous brain activity crossing the threshold for conscious access (Carhart-Harris et al., 2014; Kometer and Vollenweider, 2018). The observation of reduced power in the alpha band for different SP supports this hypothesis, given empirical evidence showing the

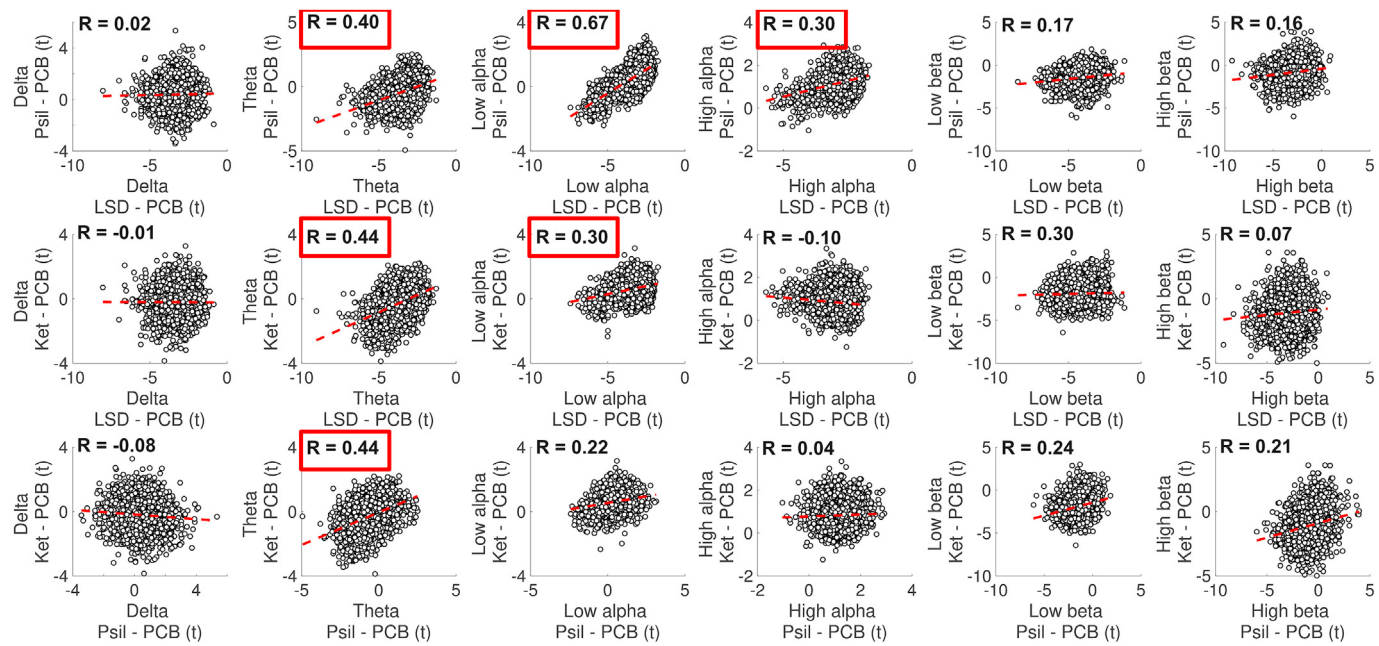


Fig. 6. Linear correlation between the changes in functional connectivity (drug – placebo). Each point represents a pair of the 90 ROIs; with its x and y axis coordinates indicating the functional connectivity change (Student's t-values) for all pairs of drugs and frequency bands. Dashed red lines indicate the best linear fit in the least-squares sense. Pearson's linear correlation coefficients (R) are provided as insets. PCB: placebo; LSD: lysergic acid diethylamide; Psil: psilocybin; Ket: ketamine. Correlations presenting high effect sizes are highlighted in red.

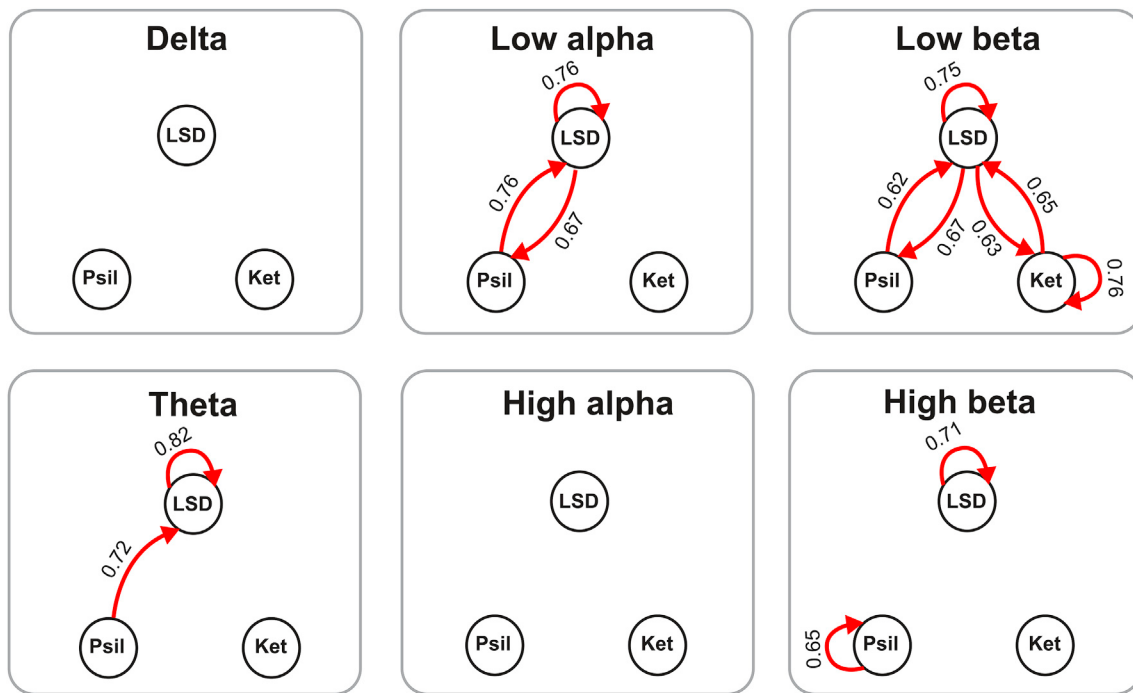


Fig. 7. Generalization of machine learning classifiers to distinguish drug vs. placebo based on the functional connectivity computed using the envelopes of the delta, theta, low and high alpha, and low and high beta bands. Red arrows indicate significant accuracy ($p < 0.05$, Benjamini-Hochberg FDR-corrected determined by 1000 classifiers with random label shuffling) of a random forest classifier trained to distinguish the drug indicated in the starting node and tested to distinguish the drug indicated in the ending node. The mean AUC values for each classifier are shown next to the corresponding arrows (e.g. a classifier trained to distinguish psilocybin from placebo in the theta band can distinguish LSD from placebo with $AUC = 0.72$ and $p < 0.05$, Benjamini-Hochberg FDR-corrected). LSD: lysergic acid diethylamide; Psil: psilocybin; Ket: ketamine.

involvement of the alpha rhythm in the suppression of irrelevant brain activity fluctuations and top-down inhibitory control processes (Klimesch et al., 2007). Our results are in line with this proposal, since the pattern of functional connectivity decreases in the low alpha band was specific to LSD and psilocybin, and did not allow accurate generalization of machine

learning classifiers to the ketamine data. Furthermore, the functional connectivity profile of individual occipital ROIs allowed to distinguish LSD from placebo, as well as the generalization towards the classification of psilocybin vs. placebo, and vice-versa.

LSD produced significant connectivity decreases in all frequency

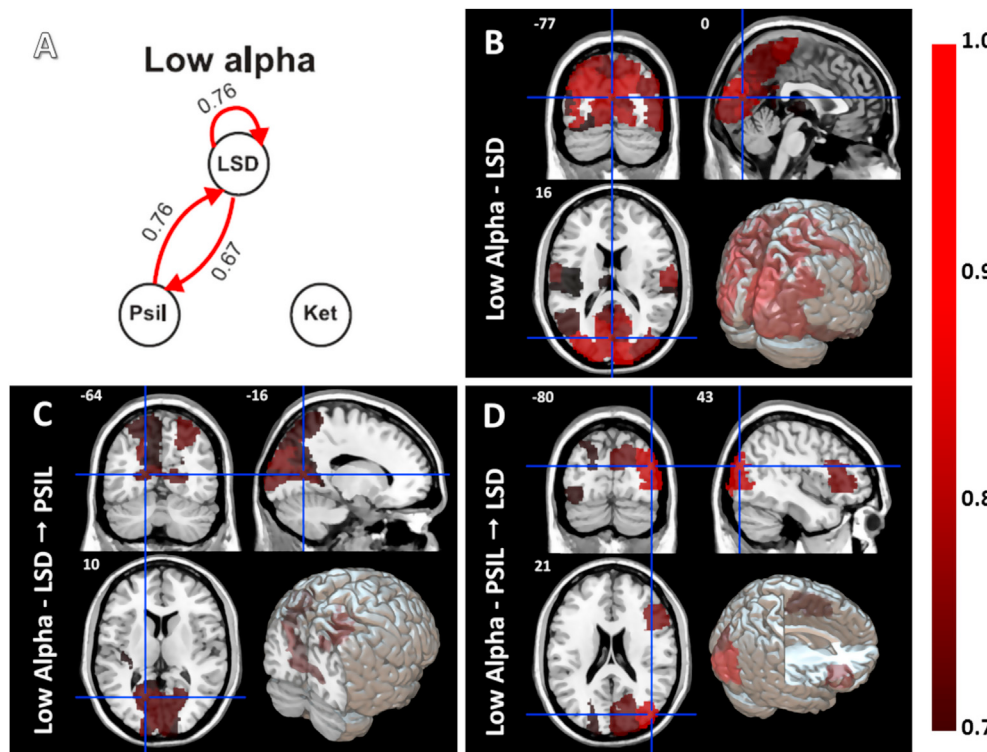


Fig. 8. Mapping of local classification accuracies based on functional connectivity of the low alpha envelope. A) Summary of the classifier accuracies in the low alpha band (reproduced from Fig. 7). B) Brain areas whose local functional connectivity features yielded significant accuracy for random forest classifiers trained and evaluated with LSD data and the corresponding placebo. C) Mapping of areas whose local functional connectivity features allowed the generalization from LSD to psilocybin data. D) Mapping of areas whose local functional connectivity features allowed the generalization from psilocybin to LSD data (the color code indicates the AUC of the classifiers).

bands, as revealed by mass univariate statistical tests. This reduction is opposite to the reported functional connectivity increases measured with fMRI between some regions under the acute effects of LSD and psilocybin (Carhart-Harris, Erritzoe et al. 2012) Driesen et al. (2013); Tagliazucchi et al. (2016) (Carhart-Harris, Muthukumaraswamy et al. 2016). This could be related to the association between the BOLD signal and gamma band activity (Logothetis et al., 2001; Scheeringa et al., 2011), which was excluded from our analyses due to muscular artifacts. Generally, LSD resulted in the most widespread and marked changes in spectral power and functional connectivity. The results of our analysis based on multivariate machine learning classifiers revealed similar patterns of disrupted functional connectivity for psilocybin and ketamine in certain frequency bands, suggesting that the differences with LSD in these bands are of a quantitative nature, possibly reflecting dose-dependent effects as well as the specific pharmacology of this drug (Wacker et al., 2017).

Our findings are limited by the exclusion from the analyses of oscillatory activity in the gamma band. Since this frequency band is prone to reflect muscular artifacts (Muthukumaraswamy, 2013), which are especially manifest under the acute effects of SP (Barbeau and Rossignol, 1990), we decided to exclude this activity from our analyses. Considering that previous neuroimaging studies of sub-anesthetic doses of ketamine reported changes in the gamma band (Lazarewicz et al., 2009; Muthukumaraswamy et al., 2015) and that the fMRI BOLD signal primarily reflects activity on this band (Logothetis et al., 2001; Scheeringa et al., 2011), future studies should address the challenge of recording sufficiently clean gamma activity under the effects of SP to allow the comparison with ketamine and with the results of fMRI experiments.

In summary, we introduced a framework to assess whether the information that enables the distinction between activity recorded during the acute effects of certain psychoactive drugs and that obtained during the placebo condition can be generalized with significant accuracy to other drugs. This method could be valuable for the study of new substances whose mechanisms and effects remain to be fully understood. New compounds could be characterized by the similarity of the brain activity elicited by them and by substances with known neurochemistry.

More generally, the application of this framework to the activity elicited by psychoactive drugs is a particular case of its application towards examining convergences and divergences in different brain states.

Acknowledgments

CP was supported by a postdoctoral fellowship of the National Scientific and Technical Research Council (Argentina). FZ was supported by a doctoral fellowship of the National Scientific and Technical Research Council (Argentina). We thank Christopher Timmermann for many insightful discussions.

This work was supported by the Argentine Consejo Nacional de Innovacion, Ciencia y Tecnologia.

References

- Abraham, A., Pedregosa, F., Eickenberg, M., Gervais, P., Mueller, A., Kossaifi, J., Gramfort, A., Thirion, B., Varoquaux, G., 2014. Machine learning for neuroimaging with scikit-learn. *Front. Neuroinf.* 8, 14.
- Aghajanian, G.K., Marek, G.J., 1997. Serotonin induces excitatory postsynaptic potentials in apical dendrites of neocortical pyramidal cells. *Neuropharmacology* 36, 589–599. [https://doi.org/10.1016/S0028-3908\(97\)00051-8](https://doi.org/10.1016/S0028-3908(97)00051-8).
- Aghajanian, G.K., Marek, G.J., 1999. Serotonin, via 5-HT2A receptors, increases EPSCs in layer V pyramidal cells of prefrontal cortex by an asynchronous mode of glutamate release. *Brain Res.* 825, 161–171. [https://doi.org/10.1016/S0006-8993\(99\)01224-X](https://doi.org/10.1016/S0006-8993(99)01224-X).
- Anis, N.A., Berry, S.C., Burton, N.R., Lodge, D., 1983. The dissociative anaesthetics, ketamine and phencyclidine, selectively reduce excitation of central mammalian neurones by N-methyl-aspartate. *Br. J. Pharmacol.* 79, 565–575. <https://doi.org/10.1111/j.1476-5381.1983.tb11031.x>.
- Barbeau, H., Rossignol, S., 1990. The effects of serotonergic drugs on the locomotor pattern and on cutaneous reflexes of the adult chronic spinal cat. *Brain Res.* 514, 55–67. [https://doi.org/10.1016/0006-8993\(90\)90435-E](https://doi.org/10.1016/0006-8993(90)90435-E).
- Barrett, F.S., Preller, K.H., Herdener, M., Janata, P., Vollenweider, F.X., 2018. Serotonin 2A receptor signaling underlies LSD-induced alteration of the neural response to dynamic changes in music. *Cerebr. Cortex* 28 (11), 3939–3950.
- Breiman, L., 2001. Random forests. *Mach. Learn.* 45 (1), 5–32.
- Carhart-Harris, R.L., Erritzoe, D., Williams, T., Stone, J.M., Reed, L.J., Colasanti, A., Tyacke, R.J., Leech, R., Malizia, A.L., Murphy, K., Hobden, P., Evans, J., Feilding, A., Wise, R.G., Nutt, D.J., 2012a. Neural correlates of the psychedelic state as determined by fMRI studies with psilocybin. *Proc. Natl. Acad. Sci.* 109, 2138–2143. <https://doi.org/10.1073/pnas.1119598109>.
- Carhart-Harris, R.L., Leech, R., Erritzoe, D., Williams, T.M., Stone, J.M., Evans, J., Sharp, D.J., Feilding, A., Wise, R.G., Nutt, D.J., 2012b. Functional connectivity

- measures after psilocybin inform a novel hypothesis of early psychosis. *Schizophr. Bull.* 39, 1343–1351. <https://doi.org/10.1093/schbul/sbs117>.
- Carhart-Harris, R.L., Leech, R., Hellyer, P.J., Shanahan, M., Feilding, A., Tagliazucchi, E., Chialvo, D.R., Nutt, D., 2014. The entropic brain: a theory of conscious states informed by neuroimaging research with psychedelic drugs. *Front. Hum. Neurosci.* 8, 20. <https://doi.org/10.3389/fnhum.2014.00020>.
- Carhart-Harris, R.L., Muthukumaraswamy, S., Roseman, L., Kaelen, M., Droog, W., Murphy, K., Tagliazucchi, E., Schenberg, E.E., Nest, T., Orban, C., Leech, R., Williams, L.T., Williams, T.M., Bolstridge, M., Sessa, B., McGonigle, J., Sereno, M.I., Nichols, D., Hellyer, P.J., Hobden, P., Evans, J., Singh, K.D., Wise, R.G., Curran, H.V., Feilding, A., Nutt, D.J., 2016. Neural correlates of the LSD experience revealed by multimodal neuroimaging. *Proc. Natl. Acad. Sci.* 113, 201518377. <https://doi.org/10.1073/pnas.1518377113>.
- Daumann, J., Wagner, D., Heeckeren, K., Neukirch, A., Thiel, C., Gouzoulis-Mayfrank, E., 2010. Neuronal correlates of visual and auditory alertness in the DMT and ketamine model of psychosis. *J. Psychopharmacol.* 24, 1515–1524. <https://doi.org/10.1177/0269881109103227>.
- Deakin, J.F., Lees, J., McKie, S., Hallak, J.E., Williams, S.R., Dursun, S.M., 2008. Glutamate and the neural basis of the subjective effects of ketamine: a pharmacomagnetic resonance imaging study. *Arch. Gen. Psychiatr.* 65 (2), 154–164.
- Dos Santos, R.G., Osório, F.L., Crippa, J.A.S., Hallak, J.E.C., 2016. Classical hallucinogens and neuroimaging: a systematic review of human studies: hallucinogens and neuroimaging. *Neurosci. Biobehav. Rev.* 71, 715–728.
- Driesen, N.R., McCarthy, G., Bhagwagar, Z., Bloch, M., Calhoun, V., D'Souza, D.C., Gueorguieva, R., He, G., Ramachandran, R., Suckow, R.F., Anticevic, A., Morgan, P.T., Krystal, J.H., 2013. Relationship of resting brain hyperconnectivity and schizophrenia-like symptoms produced by the NMDA receptor antagonist ketamine in humans. *Mol. Psychiatry* 18, 1199–1204. <https://doi.org/10.1038/mp.2012.194>.
- Engel, A.K., Gerloff, C., Hilgetag, C.C., Nolte, G., 2013. Intrinsic Coupling Modes: multiscale interactions in ongoing brain activity. *Neuron* 80, 867–886. <https://doi.org/10.1016/j.neuron.2013.09.038>.
- Glennon, R.A., Titeler, M., McKenney, J.D., 1984. Evidence for 5-HT₂ involvement in the mechanism of action of hallucinogenic agents. *Life Sci.* 35 (25), 2505–2511.
- González-Maeso, J., Weisstaub, N.W., Zhou, M., Chan, P., Ivic, L., Ang, R., Lira, A., Bradley-Moore, M., Ge, Y., Zhou, Q., Sealfon, S.C., Gingrich, J.A., 2007. Hallucinogens recruit specific cortical 5-HT_{2A} receptor-mediated signaling pathways to affect behavior. *Neuron* 53, 439–452. <https://doi.org/10.1016/j.neuron.2007.01.008>.
- Halberstadt, A.L., 2015. Recent advances in the neuropsychopharmacology of serotonergic hallucinogens. *Behav. Brain Res.* 277, 99–120. <https://doi.org/10.1016/j.bbr.2014.07.016>.
- Hanks, J.B., González-Maeso, J., 2013. Animal models of serotonergic psychedelics. *ACS Chem. Neurosci.* 4 (1), 33–42.
- Hipp, J.F., Hawellek, D.J., Corbetta, M., Siegel, M., Engel, A.K., 2012. Large-scale cortical correlation structure of spontaneous oscillatory activity. *Nat. Neurosci.* 15 (6), 884–890.
- Homayoun, H., Moghaddam, B., 2007. NMDA receptor hypofunction produces opposite effects on prefrontal cortex interneurons and pyramidal neurons. *J. Neurosci.* 27, 11496–11500. <https://doi.org/10.1523/JNEUROSCI.2213-07.2007>.
- Kapur, S., Seeman, P., 2002. NMDA receptor antagonists ketamine and PCP have direct effects on the dopamine D(2) and serotonin 5-HT(2) receptors—implications for models of schizophrenia. *Mol. Psychiatry* 7 (8), 837–844.
- Klimesch, W., Sauseng, P., Hanslmayr, S., 2007. EEG alpha oscillations: the inhibition-timing hypothesis. *Brain Res. Rev.* 53, 63–88. <https://doi.org/10.1016/j.brainresrev.2006.06.003>.
- Kometer, M., Vollenweider, F.X., 2018. Serotonergic hallucinogen-induced visual perceptual alterations. *Behav. Neurobiol. Psychedelic Drugs* 36, 257–282.
- Kometer, M., Pokorny, T., Seifritz, E., Vollenweider, F.X., 2015. Psilocybin-induced spiritual experiences and insightfulness are associated with synchronization of neuronal oscillations. *Psychopharmacology (Berlin)* 232, 3663–3676. <https://doi.org/10.1007/s00213-015-4026-7>.
- Kraehenmann, R., Pokorny, D., Aicher, H., Preller, K.H., Pokorny, T., Bosch, O.G., Seifritz, E., Vollenweider, F.X., 2017a. LSD increases primary process thinking via serotonin 2A receptor activation. *Front. Pharmacol.* 8, 814.
- Kraehenmann, R., Pokorny, D., Vollenweider, F.X., 2017b. Dreamlike effects of LSD on waking imagery in humans depend on serotonin 2A receptor activation. *Psychopharmacology (Berlin)* 234 (13), 2031–2046.
- Krystal, J.H., Sanacora, G., Duman, R.S., 2013. Rapid-acting glutamatergic antidepressants: the path to ketamine and beyond. *Biol. Psychiatry* 73 (12), 1133–1141.
- Laufs, H., Krakow, K., Sterzer, P., Eger, E., Beyerle, A., Salek-Haddadi, A., Kleinschmidt, A., 2003. Electroencephalographic signatures of attentional and cognitive default modes in spontaneous brain activity fluctuations at rest. *Proc. Natl. Acad. Sci.* 100, 11053–11058. <https://doi.org/10.1073/pnas.1831638100>.
- Lazarewicz, M.T., Ehrlichman, R.S., Maxwell, C.R., Gandal, M.J., Finkel, L.H., Siegel, S.J., 2009. Ketamine modulates theta and gamma oscillations. *J. Cogn. Neurosci.* 22, 1452–1464. <https://doi.org/10.1162/jocn.2009.21305>.
- Lebedev, A.V., Lövdén, M., Rosenthal, G., Feilding, A., Nutt, D.J., Carhart-Harris, R.L., 2015. Finding the self by losing the self: neural correlates of ego-dissolution under psilocybin. *Hum. Brain Mapp.* 36, 3137–3153. <https://doi.org/10.1002/hbm.22833>.
- Lebedev, A.V., Kaelen, M., Lövdén, M., Nilsson, J., Feilding, A., Nutt, D.J., Carhart-Harris, R.L., 2016. LSD-induced entropic brain activity predicts subsequent personality change. *Hum. Brain Mapp.* 37, 3203–3213. <https://doi.org/10.1002/hbm.23234>.
- Logothetis, N.K., Pauls, J., Augath, M., Trinath, T., Oeltermann, A., 2001. Neurophysiological investigation of the basis of the fMRI signal. *Nature* 412, 150–157. <https://doi.org/10.1038/35084005>.
- Millière, R., 2017. Looking for the self: phenomenology, neurophysiology and philosophical significance of drug-induced ego dissolution. *Front. Hum. Neurosci.* 11, 1–22. <https://doi.org/10.3389/fnhum.2017.00245>.
- Moghaddam, B., Adams, B., Verma, A., Daly, D., 1997. Activation of glutamatergic neurotransmission by ketamine: a novel step in the pathway from NMDA receptor blockade to dopaminergic and cognitive disruptions associated with the prefrontal cortex. *J. Neurosci.* 17, 2921–2927. [https://doi.org/10.1016/S0091-3057\(93\)90217-H](https://doi.org/10.1016/S0091-3057(93)90217-H).
- Muthukumaraswamy, S.D., 2013. High-frequency brain activity and muscle artifacts in MEG/EEG: a review and recommendations. *Front. Hum. Neurosci.* 7, 1–11. <https://doi.org/10.3389/fnhum.2013.00138>.
- Muthukumaraswamy, S.D., Carhart-Harris, R.L., Moran, R.J., Brookes, M.J., Williams, T.M., Erritzoe, D., Sessa, B., Papadopoulos, A., Bolstridge, M., Singh, K.D., Feilding, A., Friston, K.J., Nutt, D.J., 2013. Broadband cortical desynchronization underlies the human psychedelic state. *J. Neurosci.* 33, 15171–15183. <https://doi.org/10.1523/JNEUROSCI.2063-13.2013>.
- Muthukumaraswamy, S.D., Shaw, A.D., Jackson, L.E., Hall, J., Moran, R., Saxena, N., 2015. Evidence that subanesthetic doses of ketamine cause sustained disruptions of NMDA and AMPA-mediated frontoparietal connectivity in humans. *J. Neurosci.* 35, 11694–11706. <https://doi.org/10.1523/JNEUROSCI.0903-15.2015>.
- Nichols, D.E., 2004. Hallucinogens. *Pharmacol. Ther.* 101, 131–181. <https://doi.org/10.1016/j.jpharmthera.2003.11.002>.
- Niesters, M., Khalili-Mahani, N., Martini, C., Aarts, L., van Gerven, J., van Buchem, M.A., Dahan, A., Rombouts, S., 2012. Effect of subanesthetic ketamine on intrinsic functional brain connectivity. *Anesthesiology* 117, 868–877. <https://doi.org/10.1097/ALN.0b013e31826a0db3>.
- Nozinger, E., 2000. Towards a neurobiology of dysfunctional arousal in depression: the relationship between beta EEG power and regional cerebral glucose metabolism during NREM sleep. *Psychiatry Res. Neuroimaging* 98, 71–91. [https://doi.org/10.1016/S0925-4927\(00\)00045-7](https://doi.org/10.1016/S0925-4927(00)00045-7).
- Nolte, G., 2003. The magnetic field lead theorem in the quasi-static approximation and its use for magnetoencephalography forward calculation in realistic volume conductors. *Phys. Med. Biol.* 48 (22), 3637–3652.
- Oostenveld, R., Fries, P., Maris, E., Schoffelen, J.-M., 2011. FieldTrip: open source software for advanced analysis of MEG, EEG, and invasive electrophysiological data. *Comput. Intell. Neurosci.* 1–9. <https://doi.org/10.1155/2011/156869>, 2011.
- Palhano-Fontes, F., Andrade, K.C., Tofoli, L.F., Jose, A.C.S., Crippa, A.S., Hallak, J.E.C., Ribeiro, S., De Araújo, D.B., 2015. The psychedelic state induced by Ayahuasca modulates the activity and connectivity of the Default Mode Network. *PLoS One* 10, 1–13. <https://doi.org/10.1371/journal.pone.0118143>.
- Park, S.W., Noh, H.J., Kim, J.M., Kim, B., Cho, S.I., Kim, Y.S., Woo, N.S., Kim, S.H., Bae, Y.M., 2016. Facilitation of serotonin-induced contraction of rat mesenteric artery by ketamine. *KOREAN J. PHYSIOL. PHARMACOL.* 20 (6), 605–611.
- Passingham, R.E., Stephan, K.E., Kötter, R., 2002. The anatomical basis of functional localization in the cortex. *Nat. Rev. Neurosci.* 3 (8), 606–616.
- Pomarol-Clotet, E., Honey, G.D., Murray, G.K., Corlett, P.R., Absalom, A.R., Lee, M., McKenna, P.J., Bullmore, E.T., Fletcher, P.C., 2006. Psychological effects of ketamine in healthy volunteers: phenomenological study. *Br. J. Psychiatry* 189 (2), 173–179.
- Preller, K.H., Vollenweider, F.X., 2018. Phenomenology, structure, and dynamic of psychedelic states. *Behav. Neurobiol. Psychedelic Drugs* 36, 221–256.
- Preller, K.H., Herdener, M., Pokorny, T., Planzer, A., Krahenmann, R., Stämpfli, P., Liechti, M.E., Seifritz, E., Vollenweider, F.X., 2017. The fabric of meaning and subjective effects in LSD-induced states depend on serotonin 2A receptor activation. *Curr. Biol.* 27 (3), 451–457.
- Preller, K.H., Burt, J.B., Ji, J.L., Schleifer, C.H., Atkinson, B.D., Stämpfli, P., Seifritz, E., Repovs, G., Krystal, J.H., D. q., Vollenweider, F.X., Anticevic, A., 2018. Changes in global and thalamic brain connectivity in LSD-induced altered states of consciousness are attributable to the 5-HT_{2A} receptor. *Epilepsia* 7.
- Qin, P., Northoff, G., 2011. How is our self related to midline regions and the default-mode network? *Neuroimage* 57, 1221–1233. <https://doi.org/10.1016/j.neuroimage.2011.05.028>.
- Ray, T.S., 2010. Psychedelics and the human receptorome. *PLoS One* 5 (2) e9019.
- Riba, J., Anderer, P., Morte, A., Urbano, G., Jané, F., Saletu, B., Barbanjo, M.J., 2002. Topographic pharmaco-EEG mapping of the effects of the South American psychoactive beverage ayahuasca in healthy volunteers. *Br. J. Clin. Pharmacol.* 53, 613–628. <https://doi.org/10.1046/j.1365-2125.2002.01609.x>.
- Riba, J., Anderer, P., Saletu, B., Barbanjo, M.J., 2004. Effects of the South American psychoactive beverage Ayahuasca on regional brain electrical activity in humans: a functional neuroimaging study using low-resolution electromagnetic tomography. *Neuropsychobiology* 50, 89–101. <https://doi.org/10.1159/000077946>.
- Rickli, A., Luethi, D., Reinis, J., Buchy, D., Hoener, M.C., Liechti, M.E., 2015. Receptor interaction profiles of novel N-2-methoxybenzyl (NBOMe) derivatives of 2,5-dimethoxy-substituted phenethylamines (2C drugs). *Neuropharmacology* 99, 546–553.
- Rickli, A., Moning, O.D., Hoener, M.C., Liechti, M.E., 2016. Receptor interaction profiles of novel psychoactive tryptamines compared with classic hallucinogens. *Eur. Neuropsychopharmacol.* 26 (8), 1327–1337.
- Roseman, L., Leech, R., Feilding, A., Nutt, D.J., Carhart-Harris, R.L., 2014. The effects of psilocybin and MDMA on between-network resting state functional connectivity in healthy volunteers. *Front. Hum. Neurosci.* 8, 204. <https://doi.org/10.3389/fnhum.2014.00204>.
- Schartner, M.M., Carhart-Harris, R.L., Barrett, A.B., Seth, A.K., Muthukumaraswamy, S.D., 2017. Increased spontaneous MEG signal diversity for psychoactive doses of

- ketamine, LSD and psilocybin. *Sci. Rep.* 7, 46421. <https://doi.org/10.1038/strep46421>.
- Scheeringa, R., Fries, P., Petersson, K.-M., Oostenveld, R., Grothe, I., Norris, D.G., Hagoort, P., Bastiaansen, M.C.M., 2011. Neuronal dynamics underlying high- and low-frequency EEG oscillations contribute independently to the human BOLD signal. *Neuron* 69, 572–583. <https://doi.org/10.1016/j.neuron.2010.11.044>.
- Scheidegger, M., Walter, M., Lehmann, M., Metzger, C., Grimm, S., Boeker, H., Boesiger, P., Henning, A., Seifritz, E., 2012. Ketamine decreases resting state functional network connectivity in healthy subjects: implications for antidepressant drug action. *PLoS One* 7, 1–9. <https://doi.org/10.1371/journal.pone.0044799>.
- Shcherbinin, S., Doyle, O., Zelaya, F.O., de Simoni, S., Mehta, M.A., Schwarz, A.J., 2015. Modulatory effects of ketamine, risperidone and lamotrigine on resting brain perfusion in healthy human subjects. *Psychopharmacology (Berlin)* 232 (21–22), 4191–4204.
- Stahl, S.M., 2013. Mechanism of action of ketamine. *CNS Spectr.* 18, 171–174. <https://doi.org/10.1017/S109285291300045X>.
- Tagliazucchi, E., Carhart-Harris, R., Leech, R., Nutt, D., Chialvo, D.R., 2014. Enhanced repertoire of brain dynamical states during the psychedelic experience. *Hum. Brain Mapp.* 35, 5442–5456. <https://doi.org/10.1002/hbm.22562>.
- Tagliazucchi, E., Roseman, L., Kaelen, M., Orban, C., Muthukumaraswamy, S.D., Murphy, K., Laufs, H., Leech, R., McGonigle, J., Crossley, N., Bullmore, E., Williams, T., Bolstridge, M., Feilding, A., Nutt, D.J., Carhart-Harris, R., 2016. Increased global functional connectivity correlates with LSD-induced ego dissolution. *Curr. Biol.* 26, 1043–1050. <https://doi.org/10.1016/j.cub.2016.02.010>.
- Titeler, M., Lyon, R.A., Glennon, R.A., 1988. Radioligand binding evidence implicates the brain 5-HT2 receptor as a site of action for LSD and phenylisopropylamine hallucinogens. *Psychopharmacology (Berlin)* 94 (2), 213–216.
- Tzourio-Mazoyer, N., Landeau, B., Papathanassiou, D., Crivello, F., Etard, O., Delcroix, N., Mazoyer, B., Joliot, M., 2002. Automated anatomical labeling of activations in SPM using a macroscopic anatomical parcellation of the MNI MRI single-subject brain. *Neuroimage* 15 (1), 273–289.
- Van Veen, B.D., van Dronkelaar, W., Yuchtman, M., Suzuki, A., 1997. Localization of brain electrical activity via linearly constrained minimum variance spatial filtering. *IEEE Trans. Biomed. Eng.* 44 (9), 867–880.
- Vollenweider, F.X., Kometer, M., 2010. The neurobiology of psychedelic drugs: implications for the treatment of mood disorders. *Nat. Rev. Neurosci.* 11, 642–651. <https://doi.org/10.1038/nrn2884>.
- Wacker, D., Wang, S., McCory, J.D., Betz, R.M., Venkatakrishnan, A.J., Levit, A., Lansu, K., Schools, Z.L., Che, T., Nichols, D.E., Shiochet, B.K., Dror, R.O., Roth, B.L., 2017. Crystal structure of an LSD-bound human serotonin receptor. *Cell* 168, 377–389. [https://doi.org/10.1016/j.cell.2016.12.033 e12](https://doi.org/10.1016/j.cell.2016.12.033).
- Zamberlan, F., Sanz, C., Martínez Vivot, R., Pallavicini, C., Erowid, F., Erowid, E., Tagliazucchi, E., 2018. The varieties of the psychedelic experience: a preliminary study of the association between the reported subjective effects and the binding affinity profiles of substituted phenethylamines and tryptamines. *Front. Integr. Neurosci.* 12, 54.